



<http://www.diva-portal.org>

Preprint

This is the submitted version of a paper presented at *IEEE International Magnetic Conference (INTERMAG)*, May 15-19, 2023, Sendai, Japan.

Citation for the original published paper:

Ibrayeva, A., Lind, E., Silva, M D., Ghorai, S., Eriksson, S. (2023)

Measurement and Modelling of Hysteresis Curves for Nonlinear Permanent Magnets at Different Inclination Angles

In: *2023 IEEE International Magnetic Conference (INTERMAG)* Institute of Electrical and Electronics Engineers (IEEE)

International Conference on Magnetism

<https://doi.org/10.1109/INTERMAG50591.2023.10265100>

N.B. When citing this work, cite the original published paper.

Permanent link to this version:

<http://urn.kb.se/resolve?urn=urn:nbn:se:uu:diva-520985>

# Measurement and Modelling of Hysteresis Curves for Nonlinear Permanent Magnets at Different Inclination Angles

Anar Ibrayeva<sup>1</sup>, *Student Member, IEEE*, Emil Lind<sup>1</sup>, *Student Member, IEEE*,  
Marcelo D. Silva<sup>1</sup>, *Student Member, IEEE*, Sagar Ghorai<sup>2</sup>, and Sandra Eriksson<sup>1</sup>, *Senior Member, IEEE*,

<sup>1</sup>Department of Electrical Engineering, Uppsala University, Uppsala 752 37, Sweden

<sup>2</sup>Department of Materials Science and Engineering, Uppsala University, Uppsala 751 03, Sweden

This paper presents the measurement results of the BH/MH curves of the Alnico 8 (LNGT40) with recoil loops and a mathematical model for the calculation of the average magnetic flux density in a cubic permanent magnet. The measurements were performed with a Vibrating Sample Magnetometer (VSM). The magnet samples have a cubic shape with 3 mm sides. BH curves in preferred (easy) and transverse directions and recoil loops were measured and compared to Alnico 9 (LNGT72) as well as to the data from the supplier. The load line of the cubic magnet in 0 A/m applied magnetic field was found. A mathematical model was developed which can approximate the  $MH_a$  curve for an applied field with an arbitrarily chosen angle between the field and easy axis, given  $MH_a$  curves for 0° and 90°. Also, a simplified general model of a cubic permanent magnet in the air and calculation results of stored energy and hysteresis losses were presented.

**Index Terms**—Alnico magnets, BH curve, Demagnetization, Permanent Magnet, Recoil Line.

## I. INTRODUCTION

THE environmental aspects and market monopoly of the rare-earth permanent magnets (PMs) push the research towards less expensive and more sustainable alternatives. A large part of NdFeB magnets is produced in China.

Alnico could be one of the alternatives for specific applications where high remanence and operational temperature are required. The disadvantage of Alnico magnets is that they cannot be exposed to high magnetic fields due to the low coercivity and nonlinearity of their BH curves.

The main purpose of this paper is to provide empirical data for modelling Alnico permanent magnets (PMs) using the finite element method (FEM), especially in simulations of electrical machines, where understanding of demagnetization behaviour is crucial for the operation [1], [2]. Also, a mathematical model of  $MH_a$  curves for different directions of applied field and a simplified PM model were developed.

The information about Alnico PMs provided by suppliers is, in most cases, limited to the second quadrant of the BH curve. Br, Hc, Hcj and recoil permeability can be insufficient for modelling Alnico magnets. In most cases, no information about recoil loops or the saturation point is provided.

More detailed data was published for some Alnico magnets but most of the articles do not specify the grade of the magnet or miss some parameters [3].

## II. THEORY

The magnetic flux density,  $B$ , of PMs can be modelled using the following equation:

$$B = \mu_0(H_i + M) \quad (1)$$

The authors would like to express their gratitude for the fruitful discussion with Peter Svedlindh from the Department of Materials Science and Engineering at Uppsala University as well as Joar Lind. This study was carried out with funding from the Swedish Research Council, Grant Number 2018-04617. This work was conducted within the StandUP for Energy strategic research framework.

$M$  is magnetization [A/m],  $\mu_0$  is the permeability of free space [H/m] and  $H_i$  is internal magnetic field [A/m], which consists of:

$$H_i = H_a - H_d \quad (2)$$

where  $H_a$  is the applied field [A/m].  $H_d$  is the demagnetizing field [A/m] and can be approximated with  $H_d = MN_d$ .  $N_d$  is the demagnetizing factor.

$N_d$  can be estimated by evaluating the steepness of the MH curve at the point of intrinsic coercivity, where the curve exhibits an anhysteretic behavior [4].

From [5], equation (1) can be rewritten as

$$B = \mu_0(H_a - H_d + M) = \mu_0(H_a - N_dM + M), [T] \quad (3)$$

The operating point of the magnet will follow a recoil loop when the magnet is partially demagnetized. The recoil loop can be approximated to a recoil line to decrease the computational time when the magnet is modelled. Results from this study aims to investigate if this approximation is valid.

## III. EXPERIMENTAL SETUP

The magnetic measurements were conducted using a vibrating sample magnetometer (VSM), model LakeShore 7404, at room temperature 295 K. The VSM is an open circuit measurement instrument that records the magnetic moment,  $m$  [emu], which can be converted to magnetization,  $M$  [A/m], by dividing  $m$  by the volume of the sample and 1000. The measurement results require "shear correction" [5], according to Eq. 1, 2 and 3.

The magnet samples of Alnico 8 LNGT40 and Alnico 9 LNGT72 were provided by Sura Magnets AB. The Alnico 8 and Alnico 9 samples have a cubic shape with a 3 mm side and weights of 200.3 mg and 197.1 mg respectively. The sample was first magnetized in the preferred (easy) direction  $< 100 >$  (See Fig. 1) until saturation, and then fully demagnetized and remagnetized in opposite direction. The sample magnetization

was evaluated and recorded at even steps of the applied field strength,  $H_a$ . The magnetic flux density,  $B$  and internal field strength,  $H_i$ , were calculated according to Eq. 3. The same measurement procedure was then repeated for Alnico 8 LNGT40 with  $30^\circ$ ,  $45^\circ$   $\langle 110 \rangle$ ,  $60^\circ$  and transverse direction  $\langle 010 \rangle$  ( $90^\circ$ ) to the preferred direction and for Alnico 9 LNGT72 with  $30^\circ$  and transverse direction  $\langle 010 \rangle$  ( $90^\circ$ ). The MH curve of  $\langle 111 \rangle$  direction is not measured due to the difficulty in mounting and fixing the sample on the rod to measure it. Apart from this, Alnico 8 sample remanence was also evaluated. At certain intervals during demagnetization, the applied field was reduced to zero, and sample remanence values were collected, before the next cycle of increasing the demagnetizing field. This was repeated until the sample was fully demagnetized. The MH curves for the three directions and the recoil lines of the preferred direction can be seen in Fig. 2 and 3.

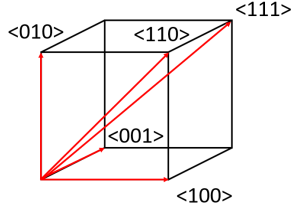


Fig. 1. Measurement directions of the cubic magnet sample

The BH curve of  $60^\circ$  direction is not presented since the demagnetizing factor of the magnet in that direction is unknown and can only be approximated. For the FEM models of Alnico magnets, it is important to obtain the hysteresis loop with an internal magnetic field.

The demagnetization with the inclined magnetic field was performed in five angles:  $15^\circ$ ,  $45^\circ$  ( $\langle 110 \rangle$ ),  $90^\circ$  ( $\langle 010 \rangle$ ),  $135^\circ$  and  $165^\circ$ .

The magnet was fully magnetized with a 14 kOe magnetic field in the easy direction, rotated to the chosen angle and demagnetized with a certain magnetic field. The remanences in both directions were measured before and after demagnetization.

#### A. Approximations and tolerances

The approximate demagnetizing factor  $N_d$  for a cube-shaped permanent magnet is  $\frac{1}{3}$  [6]. The internal magnetic field along the BH curve (demagnetization from the second to the third quadrant) changed the direction without reaching the saturation point. After analysis of the measurement data, the demagnetizing factor was changed to 0.307 and 0.312 for Alnico 8 and Alnico 9 respectively. The actual demagnetizing factors might be lower than the values that were chosen or even varying. Even if the VSM control code were set to measure the moment at 0 Oe, in reality, it was measured in a range of  $\pm 300$  Oe. The tolerance of the alignment of the magnet is  $0 \pm 5^\circ$ . There could be some tolerance of the data from the supplier of the magnets since the BH curve was digitized manually from the picture.

## IV. MEASUREMENTS AND DISCUSSION

### A. Measurement results

The relative permeability at the highest applied field during the measurement is 1.053 and 1.024 for Alnico 8 and Alnico 9 respectively. The recoil lines of Alnico 8 LNGT40 have an average slope of 2.5 mTm/kA in the easy direction and 4.18 mTm/kA in the transverse direction. The results of the measurement of the recoil permeability match the data provided by the supplier but it varies along the BH curve. The recoil permeability increases and the recoil loops become wider close to the saturation point when the sample is demagnetized (See Fig. 2). The calculated energy product  $BH_{max}$  of the Alnico 8 and Alnico 9 samples are  $56.62 \text{ kJ/m}^3$  and  $71.00 \text{ kJ/m}^3$  respectively. The relative permeability in the first quadrant of the easy direction BH curve varies from 2.11 to 61.75 for Alnico 8 and from 1.49 to 135.48. for Alnico 9.

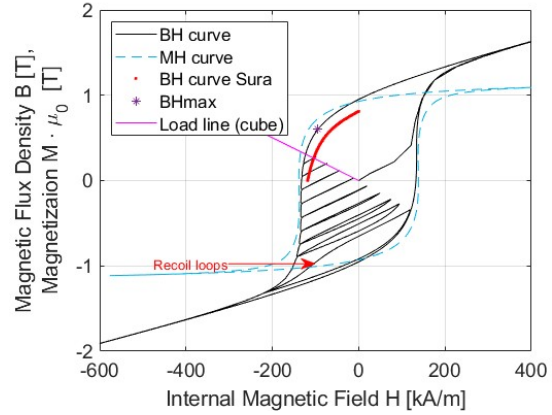


Fig. 2. MH curve and BH curve of Alnico 8 (LNGT40) in preferred (easy) direction with recoil loops

The measured BH curve of Alnico 9 is similar to the BH curve provided by the supplier (See Fig. 4). The BH curve of Alnico 8 has higher coercivity and remanence in comparison to the supplier's data (See Fig. 2). According to the measurement results, both the remanence and the coercivity decrease with the increase of the angle  $\alpha$  between the measurement direction and the easy direction (See Fig. 3).

It can be seen from Fig. 5 that even if the cubic magnet sample is magnetized only in the easy direction, VSM will measure the magnetization (Measured) that follows the  $M_{easy} \cdot \cos(\alpha)$  rule (Analytical). If the magnet was fully magnetized from the beginning and demagnetized at the inclined field, the magnetization of both directions can be approximated to

$$M_{VSM0} = M_0 + M_\alpha \cdot \cos\alpha \quad (4)$$

$$M_{VSM\alpha} = M_\alpha + M_0 \cdot \cos\alpha \quad (5)$$

The application of the magnetic field with the  $\alpha$  angle on the cubic magnet magnetized in the easy direction will affect the magnetization direction and amplitude. This field can be modelled as two components: 1) parallel or anti-parallel to the easy direction; 2) perpendicular to the easy direction. The first

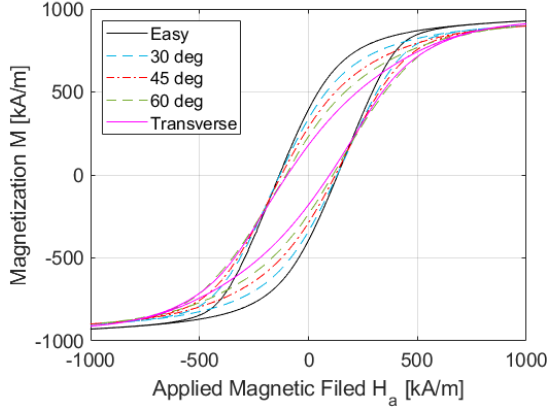


Fig. 3.  $MH_a$  curve of Alnico 8 (LNGT40) 3mm x 3mm x 3mm at  $0^\circ$ ,  $30^\circ$ ,  $45^\circ$ ,  $60^\circ$  and  $90^\circ$

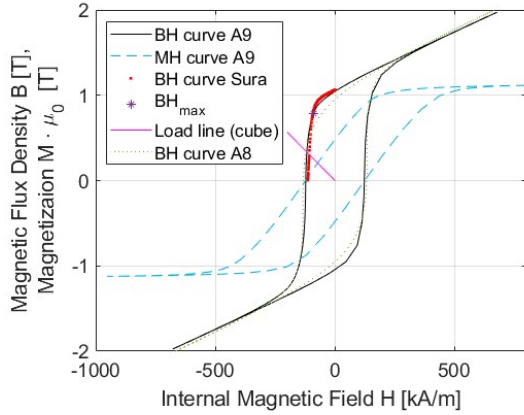


Fig. 4. BH curve of Alnico 9 (LNGT72) in preferred (easy) direction

component can demagnetize, magnetize the magnet in the easy direction and remagnetize it in the opposite direction, while the second component can only demagnetize it in the easy direction. Fig. 6 to 10 show the effect of both components for different inclination angles, as well as the  $\cos(\alpha)$  rule (Eq. 4 and 5). It can be seen that when the magnet is magnetized in  $\alpha$  direction, the magnetization of the easy direction is decreased accordingly. Fig. 10 shows the normalized sum of magnetic moments in 0 and  $\alpha$  direction  $M_{VSM0} + M_{VSM\alpha} - 1$ .

The work done per unit volume by an external field, which is stored as magnetocrystalline energy  $E_{mc}$  is

$$W = E_{mc} = \int_0^M \mu_0 H dM \quad (6)$$

Table I contains the stored energy in the material at its remanence  $M_r$  point, the difference between stored energy in the easy and transverse direction and hysteresis losses when the sample is driven through one complete cycle. The latter was calculated the same way as the stored energy but was integrated over the whole area of the MH loop.

### B. Discussion of the measurement results

One of the aims of the paper is to check if approximations of the recoil lines and demagnetisation factor are valid for

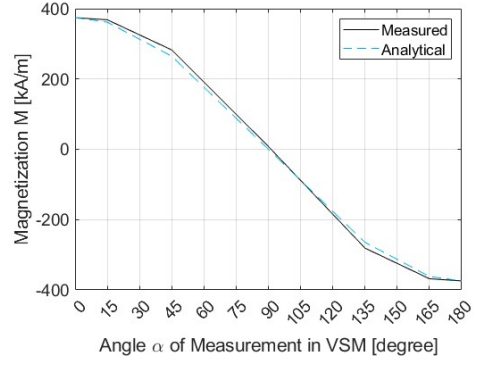


Fig. 5. Magnetization of a cube magnet sample of Alnico 8 LNGT40 magnetized in the preferred (easy) direction measured in VSM at different angles

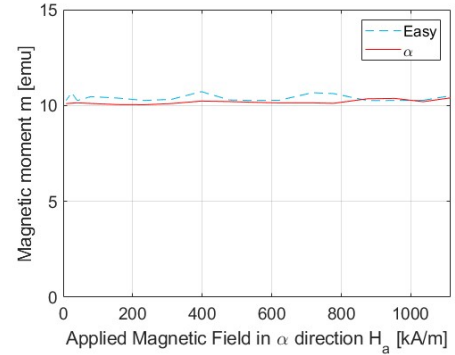


Fig. 6. Magnetic moment measured in VSM with 0 A/m applied magnetic field at  $0^\circ$  (Easy) and  $15^\circ$  ( $\alpha$ ) after experiencing  $H_a$  in  $\alpha$  direction

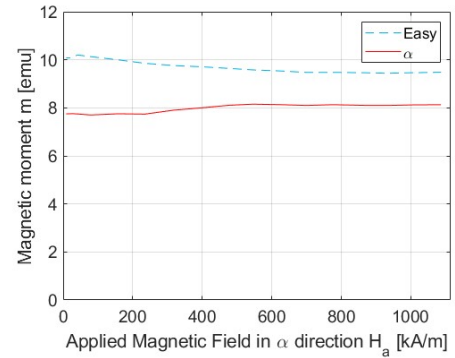


Fig. 7. Magnetic moment measured in VSM with 0 A/m applied magnetic field at  $0^\circ$  (Easy) and  $45^\circ$  ( $\alpha$ ) after experiencing  $H_a$  in  $\alpha$  direction

TABLE I  
STORED ENERGY AND HYSTERESIS LOSSES IN ALNICO 8 LNGT40 MAGNETS

	Stored energy $\frac{kJ}{m^3}$	Difference stored energy $\frac{kJ}{m^3}$	Hysteresis losses $\frac{kJ}{m^3}$	Difference hyst. losses $\frac{kJ}{m^3}$
Easy direction	135.2	51.8	514.7	243.9
Transverse direction	83.4		270.8	

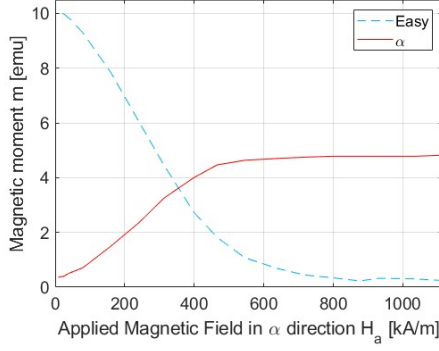


Fig. 8. Magnetic moment measured in VSM with 0 A/m applied magnetic field at  $0^\circ$  (Easy) and  $90^\circ$  ( $\alpha$ ) after experiencing  $H_a$  in  $\alpha$  direction

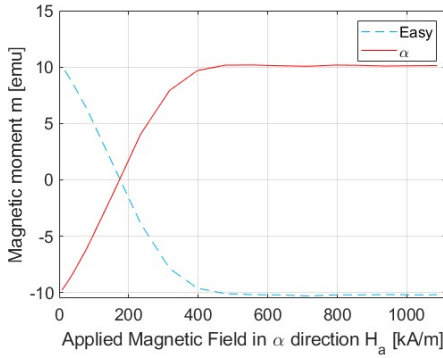


Fig. 9. Magnetic moment measured in VSM with 0 A/m applied magnetic field at  $0^\circ$  (Easy) and  $165^\circ$  ( $\alpha$ ) after experiencing  $H_a$  in  $\alpha$  direction

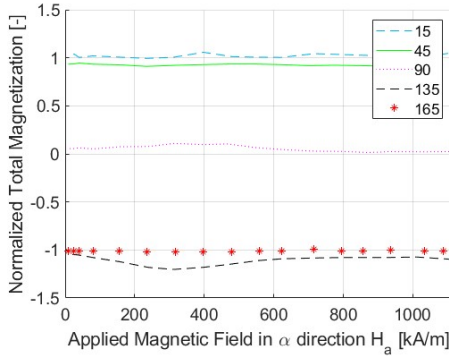


Fig. 10. Total normalized magnetization measured ( $M_{VSM0} + M_{VSM\alpha}$ ) in VSM with 0 A/m applied magnetic field after demagnetization at  $15^\circ$ ,  $45^\circ$ ,  $90^\circ$ ,  $135^\circ$  and  $165^\circ$

Alnico magnets. The recoil loops of the magnet cannot be fully measured with the cube-shaped magnet without applying a magnetizing magnetic field since the load line of the magnet without any applied magnetic field is placed too low (Fig. 2).

As shown in Fig. 2, the BH curve measured in VSM have similar to the shape of the BH curve provided by the supplier in the second quadrant but with higher remanence  $B_r$  and coercivity  $H_c$ . Alnico 9 has a better fit in comparison to Alnico 8 (Fig. 4).

When the magnetization of the transverse direction reaches

its saturation point, the magnetization of the easy direction will be 0 and vice versa. Since the demagnetizing factor and BH/MH curves of the easy and transverse direction of the magnet sample might differ, the maximum magnetization also differs. In this study, a cubic magnet sample was used. The demagnetizing factor of both easy and transverse directions was approximated to  $\frac{1}{3}$  but was corrected to 0.307 and 0.312 for Alnico 8 and Alnico 9 respectively. At  $15^\circ$  and  $45^\circ$  the shape of the sample in the magnetizing direction differ and was not found. The shape of the BH curve and the demagnetizing factor of the magnet affect the magnetization at the same time and it makes it more difficult to separate the effect of those two in the measurement results.

## V. MATHEMATICAL MODEL OF THE HYSTERESIS CURVES

### A. Hysteresis model for inclined field

The inclined field demagnetization of the cube magnet in the air can be imagined as two components: 1) magnetization in the same axis as the initial magnetization (can be both positive and negative); 2) demagnetization (will only demagnetize the magnet in the easy direction until it reaches 0).

The effect of the demagnetizing component is small and the demagnetizing factor is almost the same for a small angle inclined field demagnetization.

The operating point of the magnet and permeability in the magnetizing direction for the transverse directions and demagnetizing directions are important. The lower the  $\mu_r$  in the initial and magnetized directions, the more difficult it is to demagnetize the magnet in the easy direction and vice versa. Higher relative permeability makes both magnetization and demagnetization easier. The magnetic flux density in the easy direction will be:

$$B_{easy} = \mu_0 \cdot (H_{a\alpha} \cdot k_1 \cdot \cos\alpha - N_d \cdot M + M) \cdot k_2 \cdot \left(1 - \frac{M_{90}^{max}(H_{a\alpha}^{max})}{M_{sat90}}\right) \cdot (1 - \sin\alpha) \quad (7)$$

Both  $k_1$  and  $k_2$  are variables that are affected by the shape of the BH curve (See Eq. 9) in the easy direction, a virgin curve in the transverse direction and demagnetizing factor  $N_{d\alpha}$  at the applied magnetic field angle.  $B^{max}$  and  $H^{max}$  are the maximum magnetic flux density and the maximum magnetic field respectively that the magnet has experienced in the given direction.  $B_{sat}$  is the magnetic flux density at the saturation point at the given direction. The model can be improved in the future by finding a more accurate representation of  $k_1$  and  $k_2$  variables.

Eq. 7 can be used for the calculation of the change of magnetic flux density of the permanent magnet in the easy direction after demagnetizing it with an inclined field. The equation can be modified so the internal magnetic field is used instead of applied and could be used in FEM software to model the inclined field demagnetization of nonlinear permanent magnets. There are existing models of the inclined filed demagnetization [7] but they are for linear permanent magnets or do not take into account the demagnetization with a perpendicular magnetic field or differ from the model presented above.



### B. Mathematical model of $MH_a$ curve

There are many different methods to empirically model the hysteresis curve. One of the methods is to use the hyperbolic tangents function [8], which can approximate the upper part of the normalized  $MH_a$  curve using the equation:

$$M(H_a) = -\tanh(pH_a + c) \quad (8)$$

If instead of a first degree polynomial we expand  $pH_a + c$  into a higher degree polynomial we can get more accurate results. The polynomial  $pH_a + c$  is redefined as the following expression  $\sum_{k=1}^n p_k H_a^{k-1}$ , and inserted into Eq. 8, which gives Eq. 9.

$$M(H_a) = -\tanh\left(\sum_{k=1}^n p_k H_a^{k-1}\right) \quad (9)$$

A higher degree polynomial could yield more accurate results, but for this study  $n$  was limited to 6. Curve fitting using the nonlinear least squares method, *lsqcurvefit* in Matlab, was used to find the coefficients for the expressions using normalized measured data of  $M$  and  $H_a$ , for both  $0^\circ$  and  $90^\circ$  inclination of the applied field with regard to easy axis. The calculated coefficients,  $p_k$ , can be seen in table II.

TABLE II  
COEFFICIENTS OF THE POLYNOMIAL FOR  $MH_a$  CURVE OF ALNICO MAGNETS

	Angle ( $^\circ$ )	p1	p2	p3	p4	p5	p6
Alnico 8	0	-0.9334	-5.9525	2.4807	-1.1001	-0.9280	0.9474
	90	-0.4178	-3.8015	1.4163	-0.8440	-1.2003	0.1550
Alnico 9	0	-0.9557	-7.9958	-4.1343	1.0693	18.489	-12.192
	90	-0.1465	-3.0242	0.3755	-0.8322	-0.2521	-1.8628

The goal was then to find an expression which models the  $MH_a$  curve at an arbitrarily chosen applied field angle between  $0^\circ$  and  $90^\circ$  degrees,  $\alpha$ , using the curves and coefficients estimated for  $0^\circ$  and  $90^\circ$ . An empirical model was developed, and the results were then verified with measured data for a few chosen angles.

The empirical model that was found for a normalized  $MH$  curve for any arbitrary angle can be seen in Eq. 10.

$$M(\alpha) = -\tanh\left(\sum_{k=1}^n p_{k,0} \cos^\beta(\alpha) H_0^{k-1} + p_{k,90} (1 - \cos^\beta(\alpha)) H_{90}^{k-1}\right) \quad (10)$$

where  $n$  was set to 6 and  $\beta$  was estimated to 2.4771 using curve fitting with *lsqcurvefit*. Alnico 8 measurement data, curve fitting of the two  $MH_a$  curves,  $0^\circ$  and  $90^\circ$ , and results from the developed model for  $30^\circ$  and  $45^\circ$ , can be seen in Fig. 11.

The mathematical model approximates the  $MH_a$  curves well, especially in the second quadrant, which is usually of most interest, and minimizes the need for extensive measurements. Given the correlation between  $MH_a$  and  $BH$ , it could be possible to use this method to also construct  $BH$  curves for arbitrary angles, which can be used in for example FEM simulation tools, but since limited  $BH$  data was available this needs to be verified in further studies.

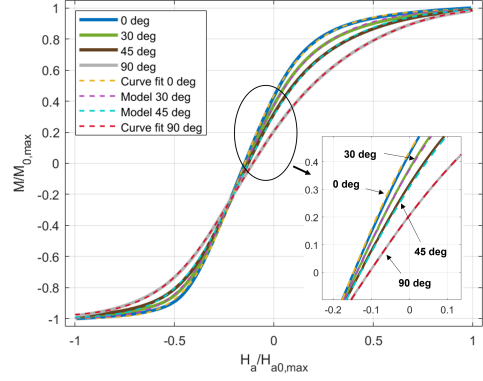


Fig. 11. Normalized demagnetization measurement data for Alnico 8 for  $0^\circ$ ,  $30^\circ$ ,  $45^\circ$  and  $90^\circ$  along with curve fitting for  $0^\circ$  and  $90^\circ$  and model estimation for  $30^\circ$  and  $45^\circ$ .

### VI. CONCLUSION

The average recoil permeability  $\mu_r$  is 1.99 but it is not constant along the  $BH$  curve. It is slightly higher closer to the saturation points when the magnet is being demagnetized. The recoil loops of Alnico 8 can be approximated to recoil lines if the magnet is operating in the second quadrant. The magnet with a smaller demagnetizing factor should be used for measuring the recoil loops. The actual demagnetizing factor of the cubic Alnico magnets is lower than  $\frac{1}{3}$  or might be even variable.

Further work should include finding  $k_1$  and  $k_2$  for the demagnetization model of Alnico PMs at different angles. The demagnetization factors at different inclination angles should be calculated.

### REFERENCES

- [1] M. Wang, B. Yu, C. Tong, G. Oiao, F. Liu, S. Yang, and P. Zheng, "Optimization on magnetization-regulation performance of a variable-flux machine with parallel permanent magnets," in *2020 IEEE 19th Biennial Conference on Electromagnetic Field Computation (CEFC)*, 2020, pp. 1–4.
- [2] C. Lee and F. Kucuk, "Variable magnet based performance improvement of pm-assisted synchronous reluctance motor," in *2022 4th Asia Energy and Electrical Engineering Symposium (AEEES)*, 2022, pp. 76–81.
- [3] P. Campbell and S. Al-Murshid, "A model of anisotropic alnico magnets for field computation," *IEEE Transactions on Magnetics*, vol. 18, no. 3, pp. 898–904, 1982.
- [4] L. K. Varga, J. Kováč, and L. Novák, "Determination of external and internal demagnetizing factors for strip-like amorphous ribbon samples," *Journal of Magnetism and Magnetic Materials*, vol. 507, p. 166845, 2020. [Online]. Available: <https://www.sciencedirect.com/science/article/pii/S030488531933077X>
- [5] B. Cullity and C. Graham, *Introduction to Magnetic Materials*, 2nd ed. John Wiley Sons, 2009.
- [6] A. Aharoni, "Demagnetizing factors for rectangular ferromagnetic prisms," *Journal of Applied Physics*, vol. 83, no. 6, pp. 3432–3434, 1998. [Online]. Available: <https://doi.org/10.1063/1.367113>
- [7] S. Ruoho, E. Dlala, and A. Arkio, "Comparison of demagnetization models for finite-element analysis of permanent-magnet synchronous machines," *IEEE Transactions on Magnetics*, vol. 43, no. 11, pp. 3964–3968, 2007.
- [8] M. Jesenik, M. Mernik, and M. Trlep, "Determination of a hysteresis model parameters with the use of different evolutionary methods for an innovative hysteresis model," *Mathematics*, vol. 8, no. 2, 2020. [Online]. Available: <https://www.mdpi.com/2227-7390/8/2/201>